Anttu, Nicklas; Kivisaari, Pyry; Chen, Yang

Tailored emission to boost open-circuit voltage in solar cells

Published in:
Journal of Physics Communications

DOI:
10.1088/2399-6528/ab1cc4

Published: 01/01/2019

Document Version
Publisher's PDF, also known as Version of record

Tailored emission to boost open-circuit voltage in solar cells

Journal of Physics Communications

PAPER

Tailored emission to boost open-circuit voltage in solar cells

Nicklas Anttu[1], Pyry Kivisaari[2] and Yang Chen[3]

[1] Department of Electronics and Nanoengineering, Aalto University, PO Box 13500, FI-00076, Aalto, Finland
[2] Engineered Nanosystems Group, Aalto University, PO Box 13500, FI-00076, Aalto, Finland
[3] Division of Solid State Physics and Nano Lund, Lund University, PO Box 118, SE-22100, Lund, Sweden

E-mail: nicklas.anttu@aalto.fi

Keywords: solar cell, emisison management, open-circuit voltage

Supplementary material for this article is available online

OPEN ACCESS

RECEIVED
11 March 2019

REVISED
23 April 2019

ACCEPTED FOR PUBLICATION
26 April 2019

PUBLISHED
20 May 2019

Abstract

Recently, a lot of research focus has been on how to make solar cells more efficient. One direction is to enhance the open-circuit voltage V_{oc} by optimizing the emission of photons in the cell, where emission is a necessary loss process due to the reciprocity between absorption and emission of light. Here, we performed a Shockley-Queisser detailed balance analysis to predict the benefit of managing emitted photons in a single-junction solar cell. First, at low internal luminescence efficiency η_{int}, non-radiative recombination dominates, and management of emitted photons plays negligible role for V_{oc}. Similarly, for an external luminescence efficiency $\eta_{ext} < 10\%$, externally emitted photons play negligible role, and V_{oc} is set either by non-radiative recombination; or parasitic absorption of internally emitted photons. For higher η_{ext}, the V_{oc} can be boosted, maximally by 15%, by restricting the external emission to match the incidence cone of the AM1.5D sun light spectrum. Such emission restriction corresponds to lower escape probability of internally emitted photons, enhances photon recycling, drops η_{ext}, and actually makes the solar cell into a worse LED. Finally, for partly diffuse incident light, by restricting the angular emission for photons in a 130 nm wavelength range around the bandgap, we predict a maximum 14% relative boost in solar cell efficiency. The results of this paper are intended to serve as a general guideline on how to utilize emission-tuning possibilities to develop highly efficient photovoltaic devices.

1. Introduction

Solar energy is a green source of energy, and solar cells could contribute a significant fraction of the world energy demand. The installed photovoltaics capacity increased from 8 to 402 GW from 2007 to 2017, showing exponential increase [1]. By the end of 2017, an equivalent of more than 40 000 solar panels were installed per hour, and solar cells supplied 1.9% of the world-wide electricity production [1]. Hence, any design improvements for better solar cell performance are expected to have noticeable impact on the global renewable energy production.

For a solar cell, one of the most important figures of merit is the efficiency η_{PV} at maximum power point, which tells us how large fraction of the incident solar energy can be converted to electrical energy [2, 3]. The efficiency can be expressed in turn as $\eta_{PV} = j_{sc} V_{oc} FF / I_{inc}$. Here, j_{sc} is the short-circuit current (density) that shows up at zero voltage bias over the solar cell, V_{oc} is the open-circuit voltage that is the maximum voltage obtained under sunlight, FF is the fill factor that gives the fraction of $j_{sc} V_{oc}$ that is extracted at the maximum power point, and I_{inc} is the incident solar intensity (see figure 1(a) for a schematic of the solar cell connected to external circuit, figure 2(a) for the absorption of sun light to produce j_{SC}, and figure 2(b) for the resulting IV curve). Therefore, to optimize the efficiency, we should aim to maximize j_{sc}, V_{oc}, and FF.

An extensive research effort has been spent on investigating how to optimize j_{sc} through varying light trapping concepts. With such concepts, the interaction of the incident light with the solar cell absorber is prolonged to enhance absorption probability [6, 7]. Another important research direction is the optimization of

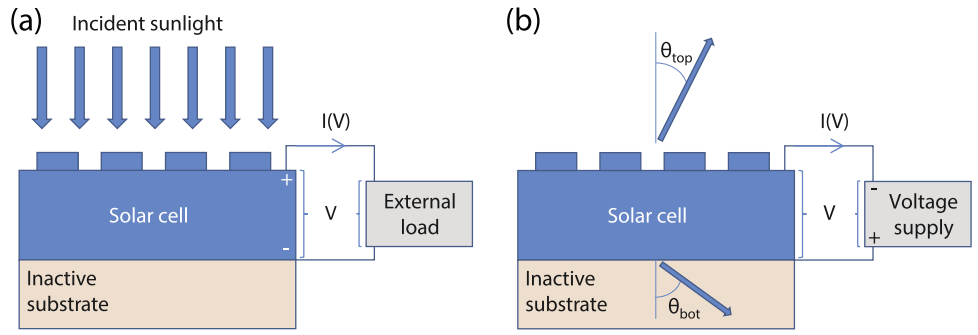

Figure 1. (a) Schematic of a solar cell, where the patterning at the top indicates a possible nanostructuring for modifying the optical properties. Here, the sunlight causes a current and a voltage in the external load. In this case, the external load receives the power $P = VI$. Note that the external load and the solar cell are biased at the same voltage. The AM1.5D solar spectrum corresponds to light incident from a small incidence cone of 2.5° half-angle around the normal incidence [4], as schematically indicated by normally incident light. (b) Emission from the solar cell at forward bias without incident sunlight. In this case, $j_{sc} = 0$ and the current is given by the recombination current in equation (1). The external voltage source biases the solar cell at voltage V. The emission to the top side is indicated by the angle θ_{top}. Here, we indicate the possibility of emission into an inactive substrate by the angle θ_{bot}.

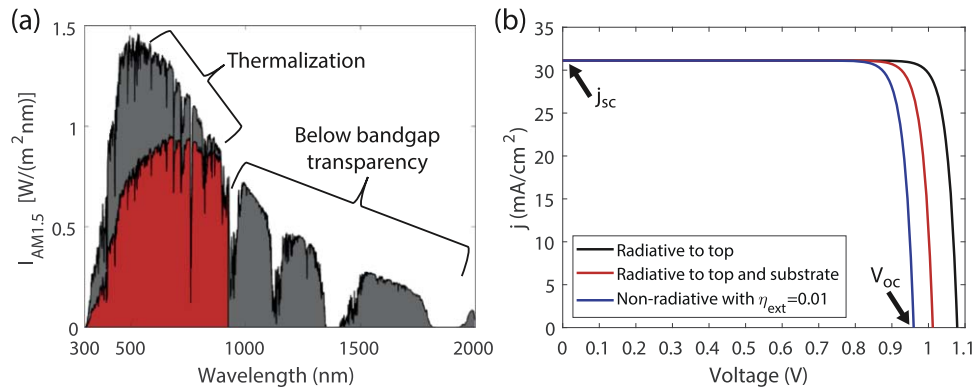

Figure 2. (a) Absorption of the 900 W m^{-2} AM1.5D direct and circumsolar spectrum by a single junction solar cell with $E_g = 1.34$ eV, corresponding to a wavelength of $\lambda_g = 925$ nm. Here, we assumed full absorption of above bandgap photons, which gives $j_{sc} = 31.3$ mA cm^{-2} from equation (2). The region marked as *Thermalization* indicates the energy that is lost due to relaxation of photogenerated carriers to the bandgap energy. (b) IV curves for a single junction solar cell with $E_g = 1.34$ eV where we assume the maximum $j_{sc} = 31.3$ mA cm^{-2}. We consider three cases of decreasing V_{oc}: (1) Emission to the full hemisphere on the top air side and no non-radiative recombination ($\eta_{int} = 1$) (black line), (2) No non-radiative recombination ($\eta_{int} = 1$) and emission to the full hemisphere both on the top air side as well as into a $n = 3.5$ refractive index substrate (red line), and (3) non-radiative recombination that gives $\eta_{ext} = 0.01$ for the case of emission to just the top side (blue line). For these three cases, we obtain $V_{oc} = 1.08$, 1.01, and 0.96 V. The fill factor shows in contrast a much smaller (relative) decrease with values of $FF = 0.89$, 0.88, and 0.88. For the efficiencies, we obtain $\eta_{PV} = 33.2\%$ for the case of no non-radiative recombination and emission only to the top side. This value is the conventional 1-sun Shockley-Queisser detailed balance limit [5]. For the case of emission to the top and bottom side, the efficiency drops to $\eta_{PV} = 30.9\%$, and for $\eta_{ext} = 0.01$, we obtain $\eta_{PV} = 29.1\%$.

V_{oc}. Both V_{oc} and FF are set by the short-circuit current and the varying recombination processes within the solar cell. Typically, V_{oc} drops much faster than FF with increasing recombination (figure 2(b) and [8]). Then, assuming optimized j_{sc}, the variation in η_{PV} is directly proportional to the variation in V_{oc}.

Hence, the recombination processes that limit V_{oc} limit directly also η_{PV}. These recombination processes can be divided into two main categories: radiative and non-radiative recombination. In radiative recombination, a photon results, for example from the recombination between an electron and a hole in a semiconductor-based solar cell. Radiative recombination is an inherent process that must exist: an absorbing solar cell must also emit photons as required by reciprocity [9]. In contrast, non-radiative recombination could in principle be minimized with perfect materials quality and optimum design of the solar cell. Thus, in an optimum solar cell, the emission of photons limits the performance.

Recently, much of the research focus has been on the possibility to optimize V_{oc} through management of emitted photons [9–17]. Especially with nanostructured solar cells, emission properties can be strongly tuned, which has the potential of boosting V_{oc} [18–20]. However, compared to the light-trapping schemes to enhance j_{sc}, optical analysis and design for boosting V_{oc} can appear more intricate.

Therefore, in this paper, we aim to establish the detailed connections between V_{oc} and the internal and external luminescence efficiencies both for radiatively and non-radiatively limited solar cells. Importantly, our work highlights in which cases tuning of emission properties can be expected to affect the solar cell efficiency.

In more detail, the radiative recombination can be analyzed through a perspective from within the active region. Here, the active region denotes the region from which photogenerated charge carriers can contribute to an external current. In this viewpoint, an internally emitted photon can either escape the solar cell and result in an externally emitted photon, be re-absorbed in the active region of the solar cell, giving rise to photon recycling, or be parasitically absorbed in an inactive region of the solar cell [16]. Alternatively, we can focus on the external properties of the emission of photons (see figure 1(b) for schematic). In this case, we look at the directional and polarization (*pol*) dependent emissivity $e_{top(bot)}(\lambda, \theta, \phi, \text{pol})$ from the solar cell to the top (bottom) side. Here, $e_{top(bot)}(\lambda, \theta, \phi, \text{pol}) = 1$ is the upper limit and corresponds to equally good emission into the direction given by the polar angles θ and ϕ as from a perfect blackbody at that wavelength λ and polarization, and $e_{top(bot)}(\lambda, \theta, \phi, \text{pol}) = 0$ indicates total restriction of that emission [18].

In an alternative approach, the solar cell performance is analyzed in terms of its LED performance, with electrical biasing over the cell to make the cell emit photons [21]. In this case, two LED quantum efficiency measures are commonly used: (1) The external luminescence efficiency η_{ext}, which is a measure of the fraction of electrically injected charge carriers that result in externally emitted photons and (2) the internal luminescence efficiency η_{int}, which gives the fraction of internal recombination that leads to internal emission of photons [21].

Recently, there has been discussion of how to manage the emitted photons to enhance V_{oc} [10–12, 14, 16, 17, 21, 22]. There have been reports indicating that the emission of photons can affect V_{oc} noticeably even when η_{int} is low [11, 23]. Such behaviour is in contradiction to the expectation from drift-diffusion based semiconductor device modelling where at low η_{int}, the photon emission can be neglected without losing accuracy of results. There, in that case, it is enough to take into account just the dominating non-radiative recombination [24, 25]. Thus, it is essential to clarify between these two opposite viewpoints for accurate solar cell analysis and design. This clarification is especially important for nanostructured solar cells, which often show low η_{int} due to the large surface-to-volume ratio that promotes additional surface recombination compared to their bulk-like counterpart. Therefore, where appropriate, we give additional comments with regard to nanostructured solar cells.

Here, we connect the internal and external emission properties, and we relate the results to η_{ext} and η_{int}. We start our presentation with a theoretical foundation for the solar cell analysis. There, we introduce the assumptions for the short-circuit current and recombination processes from which the IV-curve and V_{oc} of the solar cell can be calculated. After that, we connect analytically the V_{oc} to the external and internal luminescence efficiency. As next step, we discuss the connection between the external emissivity of the solar cell and the probability that an internally emitted photon escapes. Such connection links the internal and external management of emitted photons. Then, we discuss the effect of parasitic absorption on V_{oc}. Next, we analyze quantitatively the benefit of management of emitted photons for varying external luminescence efficiency and parasitic absorption. After that, we touch on the topic of direct versus diffuse incident light and possible benefits of managing emitted photons for partly diffuse light.

From our results, we would like to highlight that:

1. From our optics-based analysis, we show that at very low η_{int}, the non-radiative recombination sets the V_{oc}, and the way in which we manage the internally emitted photons plays no role for the solar cell efficiency η_{PV}. Thus, this viewpoint agrees with that of drift-diffusion based semiconductor device analysis where at low η_{int}, it is enough to take into account just the dominating non-radiative recombination.

2. Management of externally emitted photons becomes of practical relevance when $\eta_{ext} > 0.1$.
To enhance the solar cell efficiency, we should limit the external emission for angles outside of the cone from which sunlight is incident. That is, we should aim for $e_{top}(\theta, \phi, \text{pol}) \to 0$ for angles θ larger than the maximum incidence angle, as is conventionally proposed for external photon management [9]. This emission restriction reduces η_{ext} and hence the LED efficiency. Thus, we can make a solar cell better by making it into a worse LED. We show that such limitation of the directional emissivity corresponds to a decrease of the escape probability of the internally emitted photons. With decreasing escape probability, a larger fraction of the internally emitted photons can be re-absorbed/recycled, leading to stronger effective photogeneration inside the solar cell, which in turn allows for a larger V_{oc}.

3. On the other hand, by increasing η_{ext} through increasing materials quality in the active region, corresponding to less non-radiative recombination and higher η_{int}, both V_{oc} and η_{ext} increase. Hence, in this approach, we can make the solar cell better by making it into a better LED.

4. At 100% internal luminescence efficiency, we obtain for an example bandgap energy of 1.34 V, which maximizes the conventional single-junction 1-sun solar cell efficiency, a maximum V_{oc} of 1.24 V when we restrict the emission to a cone that matches the incident cone of 2.5° half angle of the AM1.5D direct and circumsolar sun light. Without such restriction, we find a V_{oc} of 1.08 V. When complete parasitic absorption occurs for internally emitted photons that propagate downwards, which is equivalent to emission to a refractive-index matched inactive substrate, the V_{oc} drops further to 1.01 V. In that case, angle restriction of the emission of photons to the top side gives an almost negligible maximum increase of 2 mV in V_{oc} since, for the refractive index of 3.5 assumed for the semiconductor, the loss of photons to the bottom side is $3.5^2 = 12.25$ times larger than to the top side, giving $\eta_{ext} = 0.08$.

5. When we move from the AM1.5D direct and circumsolar spectrum to the AM1.5G global tilt spectrum, approximately 10% of the light is diffusively incident. For this case, we investigated the benefit of a special type of angle restriction in the vicinity of the bandgap. To utilize the dominant, directly-incident light, we allow for full absorption within the cone of 2.5° half angle of the directly incident light also around the bandgap. Due to reciprocity between absorption and emission, there must be then full emission into that cone. However, in the vicinity of the bandgap, we restrict emission for angles outside of this cone. Such restriction leads to a decrease in j_{sc} since we don't utilize around the bandgap the diffuse light outside of this small 2.5° cone. But at the same time, we gain in V_{oc} from the limited emission of photons, which can more than compensate for the drop in j_{sc}. With such angle restriction, we predict a 1% relative boost in η_{PV} at $\eta_{ext} = 0.5$ when the emission is restricted in a 40 nm wavelength range around the bandgap, 3% at $\eta_{ext} = 0.8$ for restriction in a 60 nm wavelength range, and 14% at $\eta_{ext} = 1$ for restriction in a 130 nm wavelength range.

2. Theoretical foundations for large-area solar cells

We work with a simple diode-equation to enhance the transparency of our derivations. Where possible, we highlight the underlying assumptions. We follow in spirit the classical work by Shockley and Queisser on the detailed balance analysis of a solar cell [5], with additional comments, generalizations and clarifications as needed for our analysis. In this way, we analyze general solar cell behavior. However, note that, for a specific practical, non-ideal solar cell, additional loss-mechanisms can show up, both in j_{sc}, V_{oc} and *FF* [26]. Thus, for numerically accurate analysis of a specific, non-ideal solar cell design, for example drift-diffusion-based optoelectronics modeling might be needed [24, 25, 27–29].

2.1. Expression for IV-curve

Let us assume that we have the following relation for the IV curve of the solar cell:

$$j(V) = j_{sc} - j_{rec}(V) \tag{1}$$

where $I(V) = -A_{cell} j(V)$ is the current in the external circuit at the applied voltage V (see figure 1(a)—note that we have chosen the sign of the current within the solar cell to give positive current at short-circuit condition, but for the external circuit we use the conventional notation where positive voltage gives rise to positive current). Here, A_{cell} is the area of the solar cell, which we assume to be so large that we can neglect any effects due to the edges of the solar cell. $j(V)$ is the current (density) through the solar cell. j_{sc} is the short-circuit current (density), which results from the absorption of light in the active region of the solar cell and consecutive separation of photogenerated charge carriers, like in figure 2(a), to result in current in the external circuit, as indicated in figure 1(a). $j_{rec}(V)$ is in turn the internal recombination current (density) in the solar cell, which is in the opposite direction of j_{sc}. When the voltage is such that j_{rec} balances j_{sc} to lead to zero current in the external circuit, we are at the open-circuit voltage V_{oc} (see figure 2(b)).

Note that the above j is the externally observed average current density when considering the solar cell as a large-area black-box type solar cell. For example, in a nanowire array solar cell with axial p-n junction [30–32], the actual, local current-density in the cross-section of each nanowire is enhanced by the limited area-coverage of nanowires [25].

Importantly, here in equation (1), we assumed the superposition principle, that is, that j_{rec} only depends on the applied bias and not on photogenerated carriers (which in turn give rise to j_{sc}). Note that if strong enough recombination is present, this assumption could break down [33], like in a nanowire array solar cell with sub-optimal side-wall surface passivation of each nanowire [24].

For simplicity, we assume negligible contact resistance and other parasitic resistances and shunts, which could in principle be taken into account formally for example through additional terms in $j_{rec}(V)$. In the numerical examples, we focus on terrestrial solar cells and assume a temperature of $T = 300$ K for the solar cell.

2.2. Single junction solar cell

We focus on a single-junction semiconductor solar cell. There, the most important quantity is the bandgap energy E_g of the active region. For the numerical examples given below, we exemplify with $E_g = 1.34$ eV. Note however that our general conclusions are not dependent on this specific choice for E_g. This bandgap of 1.34 eV gives the maximum, conventional 1-sun Shockley-Queisser detailed balance efficiency [5, 18] of $\eta_{PV} = 33.2\%$ (see figure 2(b)). In comparison, for a single-junction solar cell under non-concentrated sun light, the highest measured efficiency is 29.1% [2].

2.3. Assumption for j_{sc}

For j_{sc}, we assume [18]:

$$j_{sc} = q \int_0^{\lambda_g} \frac{I_{inc}(\lambda) A_{inc}(\lambda)}{2\pi\hbar c/\lambda} d\lambda \tag{2}$$

where q is the elementary charge, $\lambda_g = 2\pi\hbar c/E_g$ with $\hbar$ the reduced Planck constant and c the speed of light in vacuum, $I_{inc}(\lambda)$ the incident solar spectrum, and $A_{inc}(\lambda)$ the absorption in the active region, averaged and weighted by the angular distribution of the incident spectrum. Here, we assume that the structure absorbs only above bandgap photons. Furthermore, we assume that each absorbed photon contributes one charge carrier to the short-circuit current. That is, we assume perfect collection of the photogenerated electron-hole pairs from the active region into short-circuit current. See figure 2(a) for the solar spectrum and its utilization.

The maximum value for j_{sc} is obtained by assuming that $A_{inc}(\lambda) = 1$ for $\lambda < \lambda_g$. Then, for the chosen bandgap of $E_g = 1.34$ eV, we obtain $j_{sc} = 31.3$ mA cm^{-2} when we use for $I_{inc}(\lambda)$ the 900 W m^{-2} AM1.5D direct and circumsolar spectrum [4]. Note that this direct and circumsolar light is incident from a cone of a small half-angle of 2.5° [4]. That is, the incidence angle is maximally 2.5° from the normal of the solar cell (note that the solar disc by itself covers a smaller disk of ≈0.26° in half-angle, but without loss of generality of our main conclusions, to focus on the AM1.5D spectrum, we use the half-angle of 2.5°). Towards the end, in section 3.6, we discuss possible impact of diffuse incident light, especially in terms of the AM1.5 G spectrum.

Note that for more accurate numerical results, it is possible to generalize the absorptance to take into account finite thickness of the absorber and below bandgap absorption in the Urbach tail [14]. However, such refinements are not expected to affect our general conclusions about the effect on V_{oc} of management of emitted photons, which is the main focus of this work.

2.4. Assumption for radiative and non-radiative recombination

To keep the derivation simple, we assume non-radiative recombination of the form $j_{nr,0}(e^{qV/kT} - 1)$ [16]. Here, $j_{nr,0}$ originates from an integration of the non-radiative recombination in the volume and on the surface of the active region. Note that the main conclusions about the effect of internal and external photon management on V_{oc} are not dependent on this exact choice for the voltage dependence, such as the ideality factor (see supporting information equation (S1), which is available online at stacks.iop.org/JPCO/3/055009/mmedia).

Then, if we assume that the radiative and non-radiative recombination are parallel pathways for recombination, the recombination current in equation (1) is given by:

$$j_{rec}(V) = (j_{em,ext,0} + j_{nr,0})(e^{qV/kT} - 1) \tag{3}$$

where $j_{em,ext,0}$ is set by the emission of photons out from the cell at thermal equilibrium (see supporting information equation (S3) and [5, 18]).

The external emission can be divided into [18]:

$$j_{em,ext,0} = j_{em,ext,0,top} + j_{em,ext,0,bot}. \tag{4}$$

Here, $j_{em,ext,0,top}$ is due to emission to the top side, and $j_{em,ext,0,bot}$ is due to emission to the bottom side, which could consist for example of an inactive substrate as is common in research-stage nanostructured solar cells [30–32], air, or a bottom mirror. The magnitudes of $j_{em,ext,0,top}$ and $j_{em,ext,0,bot}$ depend on how strong the emission is to the different emission angles and polarizations at the top and bottom side, that is, how large the emissivity $e_{top(bot)}(\lambda, \theta, \phi, \text{pol})$ is at the top (bottom) side [18] (see figure 1(b)). Furthermore, the emission depends on the refractive index n of surrounding material as n^2 [18, 34] (see also supporting information equation (S3)). Importantly, a possible emission modification, for example through nanostructuring, is captured in a modification of $e_{top(bot)}(\lambda, \theta, \phi, \text{pol})$ [18–20].

We obtain the maximum value for $j_{em,ext,0,top}$ and $j_{em,ext,0,bot}$ when we assume maximum possible emission into the full hemisphere at the top and bottom side, respectively (see supporting information equation (S3)). This maximum emission corresponds to $e_{top(bot)}(\lambda, \theta, \phi, \text{pol}) = 1$ into all external angles for $\lambda < \lambda_g$. Similarly as with the assumption of no absorption of below bandgap photons in equation (2), we assume here no emission of below bandgap photons. Then, for the bandgap of 1.34 eV, we obtain for emission to the top side, assuming a

refractive index of $n_{top} = 1$ there, $j_{em,ext,0,top} = 2.36*10^{-17}$ mA cm^{-2}. For emission into an inactive semiconductor substrate of $n_{bot} = 3.5$, we obtain $j_{em,ext,0,bot} = \left(\frac{n_{bot}}{n_{top}}\right)^2 j_{em,ext,0,top} = 2.90*10^{-16}$ mA/cm^2. Note that $j_{em,ext,0,bot}$ can be eliminated with a perfect back-mirror [10].

There are multiple implicit assumptions made in the above derivation for the recombination and emission. We assume implicitly that $E_g/q - V \gg kT$ to be able to use the Boltzmann approximation that yields the $e^{qV/kT} - 1$ dependence for the radiative recombination with constant $j_{em,ext,0}$: otherwise we need to use the Bose-Einstein distribution for the photons in the active region and the Fermi-Dirac distribution for the electrons and holes [35] (the analysis can be performed with such more complicated dependence, but we believe that the transparency of the derivations and conclusions increases when using the simpler $e^{qV/kT} - 1$ dependence). Similarly, for example degenerate doping can also lead to the need of using the Fermi-Dirac distribution. Hence, here, we limit us to cases where $E_g/q - V \gg kT$, and specifically to $E_g/q - V_{oc} \gg kT$ that actually applies for all high-efficiency solar cells to date [2]. Furthermore, we assume that the doping concentrations are low enough so that effects from degenerate doping are negligible.

Also, above, we assumed implicitly a constant quasi-Fermi level splitting through the active layer [9], so that the voltage V is constant over the whole active region. If the quasi-Fermi level splitting is not constant throughout the active region, a lower efficiency is predicted [36]. Finally, we assumed implicitly that the emissivity that applies at thermal equilibrium applies also out of equilibrium, and that emission is enhanced by the factor $e^{qV/kT}$ [9]. Hence, we assumed that all regions that emit light at thermal equilibrium are in a region from which the emission is enhanced by the factor of $e^{qV/kT}$. Thus, we then implicitly assume that there is no parasitic absorption: thermal emission from a parasitically absorbing region would not be enhanced by the voltage over the active region. Below, we discuss the topic of parasitic absorption.

2.5. Assumption for parasitic absorption

Parasitic absorption of emitted photons is an absorption process that does not create electron-hole pairs into the active region. As the amount of parasitic absorption is, in the linear optics regime, proportional to the amount of emitted photons, parasitic absorption can be included by adding a term $j_{parasitic,0}(e^{qV/kT} - 1)$ into equation (3), giving

$$j = j_{sc} - (j_{em,ext,0} + j_{parasitic,0} + j_{nr,0})(e^{\frac{qV}{kT}} - 1) \tag{5}$$

3. Results

Below, in section 3.1, we derive the dependence of V_{oc} on the external luminescence efficiency η_{ext}. In section 3.2, to complement analysis based on η_{ext}, we study the dependence of V_{oc} on the internal luminescence efficiency η_{int} and p_{esc}, the average probability that an internally generated photon escapes. There, we show that p_{esc} should be minimized to maximize V_{oc}. In section 3.3, we connect p_{esc} to the external emissivity and discuss how a minimization of p_{esc} is connected to angular restriction of external emission. Next, in section 3.4, we discuss how parasitic absorption could affect V_{oc}. Then, in section 3.5, we give numerical examples of the benefit of minimizing p_{esc} for varying η_{ext} and parasitic absorption. Finally, in section 3.6, we show the benefit of emission management in the case of partially diffuse incident light.

3.1. The dependence of V_{oc} on η_{ext}

In the continuation, we consider voltages such that $e^{qV/kT} \gg 1$, which applies for the V_{oc} of well-performing solar cells [2]—note that kT/q is approximately 26 mV at the assumed $T = 300$ K. Then equation (3), which assumes negligible parasitic absorption, simplifies to the diode equation:

$$j = j_{sc} - (j_{em,ext,0} + j_{nr,0})e^{qV/kT} \tag{6}$$

which gives

$$V = \frac{kT}{q} \ln\left(\frac{j_{sc} - j}{j_{em,ext,0} + j_{nr,0}}\right). \tag{7}$$

Since $j = 0$ at the open-circuit condition, we obtain:

$$\begin{aligned} V_{oc} &= \frac{kT}{q} \ln\left(\frac{j_{sc}}{j_{em,ext,0} + j_{nr,0}}\right) \\ &= \frac{kT}{q} \ln\left(\frac{j_{sc}}{j_{em,ext,0}}\right) + \frac{kT}{q} \ln\left(\frac{j_{em,ext,0}}{j_{em,ext,0} + j_{nr,0}}\right) \\ &= V_{oc,rad} + \frac{kT}{q} \ln(\eta_{ext}). \end{aligned} \tag{8}$$

Here $V_{oc,rad} = \frac{kT}{q} \ln\left(\frac{j_{sc}}{j_{em,ext,0}}\right)$ is the radiatively limited V_{oc} that would be obtained in the absence of non-radiative recombination, and $\eta_{ext} = \frac{j_{em,ext,0}}{j_{em,ext,0} + j_{nr,0}}$ is the external luminescence efficiency [21, 37]. That is, η_{ext} is the fraction of net recombination processes that result in the emission of a photon out from the cell, either to the top or the bottom side. See supporting information equation (S13) for how to include the emission to the bottom side instead as a parasitic absorption loss by redefining η_{ext} to include only emission to the top side.

Importantly, as seen from the first part of equation (8), to enhance V_{oc}, we can aim to decrease $j_{em,ext,0}$. In that case, η_{ext} decreases (assuming that $j_{nr,0} > 0$). Thus, with this approach, as the solar cell becomes better, it behaves as a less efficient LED. In contrast, if we increase materials quality such that $j_{nr,0}$ decreases, V_{oc} increases, η_{ext} increases, and the solar cell behaves as a more efficient LED.

3.2. The dependence of V_{oc} on η_{int} and p_{esc}

Next, we use that $j_{em,ext,0} = p_{esc} j_{em,\,int\,,0}$ (see equation (13) in Ref. [22]; and supporting information equation (S11)). Here, p_{esc} is the average probability that an internally generated photon escapes, and $j_{em,\,int\,,0}$ results from a volume-integration of the internal photon-generation rate (see supporting information equations (S7)–(S11)). We use also that $\eta_{int} = \frac{j_{em,\,int\,,0}}{j_{em,\,int\,,0} + j_{nr,0}}$. Then, we can derive:

$$\eta_{ext} = \frac{j_{em,ext,0}}{j_{em,ext,0} + j_{nr,0}} = \frac{p_{esc}\eta_{int}}{1 - (1 - p_{esc})\eta_{int}} \tag{9}$$

and

$$V_{oc} = V_{oc,rad} + \frac{kT}{q} \ln\left(\frac{p_{esc}\eta_{int}}{1 - (1 - p_{esc})\eta_{int}}\right). \tag{10}$$

For low η_{int}, the expression in equation (10) simplifies to $V_{oc} = V_{oc,rad} + \frac{kT}{q} \ln(p_{esc}\eta_{int})$. Here, at first sight, it appears that V_{oc} would increase with increasing p_{esc} if η_{int} stays fixed. However, note that there is p_{esc} dependence also in $V_{oc,rad}$ since $V_{oc,rad} = \frac{kT}{q} \ln\left(\frac{j_{sc}}{j_{em,ext,0}}\right) = \frac{kT}{q} \ln\left(\frac{j_{sc}}{p_{esc} j_{em,\,int\,,0}}\right)$. In this case of low η_{int}, $\eta_{int} \to \frac{j_{em,\,int\,,0}}{j_{nr,0}}$ and $V_{oc} \to \frac{kT}{q} \ln\left(\frac{j_{sc}}{j_{nr,0}}\right)$ as also obtained directly from the initial diode equation (equation (6)), which simplifies to $j = j_{sc} - j_{nr,0} e^{qV/kT}$ since $j_{nr,0} \gg j_{em,ext,0}$ at low η_{int}.

Hence, at very low internal luminescence efficiency, the non-radiative recombination sets the V_{oc}, and the way in which we manage the emitted photons plays no role. Note that this result that p_{esc} does not affect V_{oc} at low η_{int} can be obtained also from equation (31)** in Ref. [16] by using $\eta_{int} \to 0$ there. Thus, from this optics analysis, we obtain the same conclusion as often used in drift-diffusion modeling [24, 25]: at low η_{int}, one can neglect radiative recombination in the solar cell analysis.

More generally, for arbitrary η_{int}, equation (6) gives

$$V_{oc} = \frac{kT}{q} \ln\left(\frac{j_{sc}}{j_{em,ext,0} + j_{nr,0}}\right) = \frac{kT}{q} \ln\left(\frac{j_{sc}}{p_{esc} j_{em,\,int\,,0} + j_{nr,0}}\right). \tag{11}$$

Hence, to enhance V_{oc}, we should target to decrease p_{esc}.

To discuss in another way why a decrease in p_{esc} leads to an increase in V_{oc}, we use that $p_{recycled} = 1 - p_{esc}$ (still assuming negligible parasitic absorption). Here, $p_{recycled}$ is the probability that an internally emitted photon is re-absorbed in the active region, that is, recycled. That is, $p_{recycled}$ shows the probability that an internally emitted photon gives rise to an additional electron-hole pair in the active region. From equation (6), with $j_{em,ext,0} = p_{esc} j_{em,\,int\,,0}$, we obtain that

$$j = (j_{sc} + p_{recycled} j_{em,\,int\,,0} e^{\frac{qV}{kT}}) - (j_{em,\,int\,,0} + j_{nr,0}) e^{\frac{qV}{kT}}. \tag{12}$$

Importantly, here, the second term, $(j_{\text{em, int ,0}} + j_{\text{nr,0}})e^{\frac{qV}{kT}}$, is due to the internal recombination which does not depend on p_{esc}. Thus, we have moved the dependence on p_{esc} to the first term, $(j_{\text{sc}} + p_{\text{recycled}} j_{\text{em, int ,0}} e^{\frac{qV}{kT}})$, which is due to the photogeneration from both the external and internal illumination. Importantly, with decreasing p_{esc}, p_{recycled} increases and a larger fraction of the internally emitted photons contribute to photogeneration in the active region, allowing for a higher V_{oc}.

Note that in the above analysis, we looked at the dependence of V_{oc} on p_{esc}. That is, we assumed that p_{esc} is the only changing parameter. However, if the change in p_{esc} is accompanied for example by a simultaneous change in $j_{\text{em, int ,0}}$, we can imagine a case where $j_{\text{em, int ,0}}$ decreases, relatively, more than p_{esc} increases. Then $j_{\text{em,ext,0}} = p_{\text{esc}} j_{\text{em, int ,0}}$ decreases, and V_{oc} increases as p_{esc} increases. However, as we see it, this increase in V_{oc} does not occur due to the increase in p_{esc}, but due to the even stronger relative decrease in $j_{\text{em, int ,0}}$. Similarly, we can imagine a case where p_{esc} increases while $j_{\text{nr,0}}$ decreases in such a way that $(p_{\text{esc}} j_{\text{em, int ,0}} + j_{\text{nr,0}})$ decreases, leading to an increase in V_{oc}. However, again, the increase in V_{oc} does not occur due to the increase in p_{esc}.

3.3. The dependence of emissivity on p_{esc}

Above, we saw that to enhance V_{oc}, we should decrease p_{esc}, the probability that internally emitted photons escape the cell. This dependence on p_{esc} can be understood also from the following: (1) p_{esc} is connected to the angle dependent emissivity $e_{\text{top(bot)}}(\lambda, \theta, \phi, \text{pol})$, and (2) for optimum external emission-management, we should restrict the external emission cone to match the incidence cone [9, 18–20]. In more detail, the escape probability p_{esc} is in principle also angle dependent, but for simplicity we have used above the angle averaged p_{esc} (see supporting information equation (S10)). Technically, the external emission into a given angle results from the volume-integration of the position-dependent internal emission rate multiplied by the spatially dependent probability for escape of a photon to that external emission angle (see supporting information equation (S10)).

Therefore, there is a limit on how much we can decrease p_{esc} for fixed $j_{\text{em, int ,0}}$. In our case, this limit is given by the factor of 526 (see supporting information equation (S6)). This factor is the maximum reduction in the etendue [9] for emission when considering the direct and circumsolar AM1.5D light that is incident from the cone of 2.5° half angle [4], when starting from completely unrestricted emission to the top side with no emission to the bottom side. At this factor of 526, photons escape only to the small cone of 2.5° half angle, at full emissivity. In other words, $e_{\text{top}}(\lambda, \theta, \phi, \text{pol}) = 0$ for $\theta > 2.5°$ while $e_{\text{top}}(\lambda, \theta, \phi, \text{pol}) = 1$ for $\theta < 2.5°$. In this case, $j_{\text{em,ext,0,top}}$ is reduced by a factor of 526 to $\frac{j_{\text{em,ext,0,top}}^{\text{no-restriction}}}{526} = \frac{2.36 * 10^{-17}}{526} = 4.50{*}10^{-20}$ mA cm^{-2}, and we match the emission cone to the incidence cone. Here, $j_{\text{em,ext,0,top}}^{\text{no-restriction}}$ is the value of $j_{\text{em,ext,0,top}}$ in the case of no emission restriction.

If we attempt to decrease p_{esc} beyond this factor of 526, $e_{\text{top}}(\lambda, \theta, \phi, \text{pol})$ must decrease to below 1 for some angles $\theta < 2.5°$, that is, within the incidence cone. Since there is reciprocity between in-coupling and out-coupling of light in linear and passive optical systems [34], we have Kirchhoff's radiation law given by $e_{\text{top}}(\lambda, \theta, \phi, \text{pol}) = A(\lambda, \theta, \phi, \text{pol})$. Then, when $e_{\text{top}}(\lambda, \theta, \phi, \text{pol}) < 1$ for some angles in the incidence cone, the absorptance must drop, and the short-circuit current drops (see equation (2) where the $A(\lambda)$, which is averaged over the angles and polarization within the incidence cone, must drop). Such a drop in j_{sc} leads to a drop in efficiency if we have chosen an optimum bandgap E_{g} [9] (even if V_{oc} might increase).

In contrast, if E_{g} is below the optimum bandgap, it could in principle be possible to obtain a higher efficiency by limiting the emission completely around the bandgap wavelength. Such an energy restriction can make the effective bandgap of the solar cell appear larger and more optimized [9], depending on the strength of the non-radiative recombination [15]. Technically, in terms of the emissivity, we can introduce in this case an effective, optical bandgap wavelength $\lambda_{\text{g,eff}}$ such that $e_{\text{top}}(\lambda, \theta, \phi, \text{pol}) = 0$ for $\lambda_{\text{g,eff}} < \lambda < \lambda_{\text{g}}$, whereas for $\lambda < \lambda_{\text{g,eff}}$, $e_{\text{top}}(\lambda, \theta, \phi, \text{pol}) = 0$ for $\theta > 2.5°$ and $e_{\text{top}}(\lambda, \theta, \phi, \text{pol}) = 1$ for $\theta < 2.5°$.

3.4. Parasitic absorption

Above, we considered the case of negligible parasitic absorption. For parasitic absorption, equation (5) gives, assuming again that we consider voltages such that $qV \gg kT$,

$$j = j_{\text{sc}} - (j_{\text{em,ext,0}} + j_{\text{parasitic,0}} + j_{\text{nr,0}})e^{qV/kT} \tag{13}$$

with $j_{\text{em,ext,0}} = p_{\text{esc}} j_{\text{em, int ,0}}$ and $j_{\text{parasitic,0}} = p_{\text{parasitic}} j_{\text{em, int ,0}}$ where $p_{\text{parasitic}}$ is the probability that an internally emitted photon is parasitically absorbed. From p_{esc} and $p_{\text{parasitic}}$, we have $p_{\text{recycled}} = 1 - p_{\text{esc}} - p_{\text{parasitic}}$, the fraction of internally emitted photons that are re-absorbed, and hence recycled, in the active region (compared to the $p_{\text{recycled}} = 1 - p_{\text{esc}}$ that applied in section 3.2 for the case of negligible parasitic absorption).

Below, we assume for simplicity that the parasitic absorption affects incident photons, and hence j_{sc}, negligibly, which could be the case for example if the parasitic absorption is weak enough, happens only on the

back-side of the solar cell, or only for propagation angles from which light is not incident from. To show how parasitic absorption affects V_{oc}, from equation (13), we can solve for:

$$V_{oc} = \frac{kT}{q} \ln\left(\frac{j_{sc}}{j_{em,ext,0} + j_{parasitic,0} + j_{nr,0}}\right) = V_{oc,rad,no-parasitic} + \frac{kT}{q} \ln(\eta_{ext}). \quad (14)$$

Here,

$$V_{oc,rad,no-parasitic} = \frac{kT}{q} \ln\left(\frac{j_{sc}}{j_{em,ext,0}}\right) \quad (15)$$

is the V_{oc} that would result in the absence of parasitic absorption and non-radiative recombination, and

$$\eta_{ext} = \frac{j_{em,ext,0}}{j_{em,ext,0} + j_{parasitic,0} + j_{nr,0}} = \frac{p_{esc}\eta_{int}}{1 - p_{recycled}\eta_{int}} \quad (16)$$

where still $\eta_{int} = \frac{j_{em,\,int\,,0}}{j_{em,\,int\,,0} + j_{nr,0}}$. The $V_{oc,rad,no-parasitic}$ is a hypothetical concept: if we manage to modify the optics of the system in such a way that $j_{parasitic,0} \to 0$, the emission properties, and hence p_{esc}, and consecutively $j_{em,ext,0}$, is expected to change at the same time. Then, as seen from equation (15), due to the change in $j_{em,ext,0}$, the radiative limit for V_{oc} differs from $V_{oc,rad,no-parasitic}$. Importantly, from the first part of equation (14) we see that also with non-negligible parasitic absorption, V_{oc} is enhanced if $j_{em,ext,0}$ and hence p_{esc} is decreased.

To highlight some of the possible impacts of parasitic absorption (of internally emitted photons), let us consider the case of an optically thick active region and parasitic absorption only taking place at the bottom side for simplicity. Here, by optically thick region, we denote a region that is so thick that all above-bandgap photons are absorbed before making a round trip between the top and bottom interface. For simplicity, we adopt a ray-optics approximation where light propagates as rays in the active region. Note that in a nanostructured active region, a dedicated analysis of the Purcell effect and diffractive light scattering within the active region might be needed for more accurate analysis of the emission and absorption of light [38].

In this ray-optics case, the upper limit on parasitic absorption at the bottom interface of the cell is obtained when all the internally downward emitted photons that reach the bottom interface are absorbed there. This case gives equivalent loss in V_{oc} as emission into a refractive-index matched, inactive substrate (see for example figure 55 in [14]). Thus, in this case of the optically thick cell in the ray-optics approximation, the maximum loss in V_{oc} due to a perfectly absorbing back-mirror is the same as when having the solar cell on an inactive, refractive-index matched substrate. In terms of p_{esc} and $p_{parasitic}$, if we assume full emission to the top hemisphere (which maximizes p_{esc}), the upper limit on absorption at the bottom mirror is given by $\frac{p_{parasitic}}{p_{esc}} = (n_{cell})^2/(n_{top})^2$ where n_{cell} is the refractive index of the cell. With typical $n_{cell} = 3.5$ for a semiconductor, and by assuming $n_{top} = 1$ at the top side, we find $p_{parasitic} = 12.25{*}p_{esc}$ as the upper limit in the ray-optics approximation for the parasitic absorption in the back-mirror.

3.5. The benefit of emission management for varying η_{ext} and parasitic absorption

Here, we investigate quantitatively the benefit of management of emitted photons for the non-concentrated 900 W m^{-2} AM1.5D sunlight. Since $j_{em,ext,0} = p_{esc} j_{em,\,int\,,0}$, we choose to analyze the photon management in terms of the external emission of photons through equation (14). If we assume that the internal radiative recombination process stays constant, that is, if $j_{em,\,int\,,0}$ stays constant when $j_{em,ext,0}$ is varied, then a change in $j_{em,ext,0}$ corresponds to an equal relative change in p_{esc}. Thus, we can relate the results for varying external optical properties, in terms of $j_{em,ext,0}$, to changes in internal optical properties, in terms of p_{esc}.

In figure 3 (a), we show the benefit for V_{oc} of restricting $j_{em,ext,0}$ by the emission restriction factor $1 \leqslant F \leqslant 526$ (that can be tuned for example by varying the size of the emission cone—see supporting information equation (S6)). The results are shown for varying $\eta_{ext,init}$, which is the initial value of η_{ext} that applies at $F = 1$, that is, before any emission restriction. In more detail, we assume emission only to the top side, and use the above calculated value of $j_{em,ext,0,top} = 2.36{*}10^{-17}$ mA/cm^2 for $j_{em,ext,0}$ at $F = 1$, that is, for emission at full emissivity into the full hemisphere in the top air side. For $F > 1$, we use $j_{em,ext,0,top}/F$ for $j_{em,ext,0}$ in equation (14). Note that as we restrict the external emission with F > 1, η_{ext} drops from $\eta_{ext,init}$ (figure 3(b)), except for $\eta_{ext,init} = 1$ where $\eta_{ext} = 1$ for all F. In figures 4(a) and (b), we show the benefit of maximally restricting the emission for varying $\eta_{ext,init}$.

From these figures, we see that for an external luminescence efficiency $\eta_{ext,init} < 0.1$, there is not much point in restricting the external emission of photons: at the maximum emission restriction of $F = 526$ for the AM1.5D incident light, the gain in V_{oc} is just 2.5 mV for $\eta_{ext,init} = 0.1$, which increases to 59 mV for $\eta_{ext,init} = 0.9$. At $\eta_{ext,init} = 1$, we find a maximum increase of 162 mV in V_{oc}, which corresponds to an increase

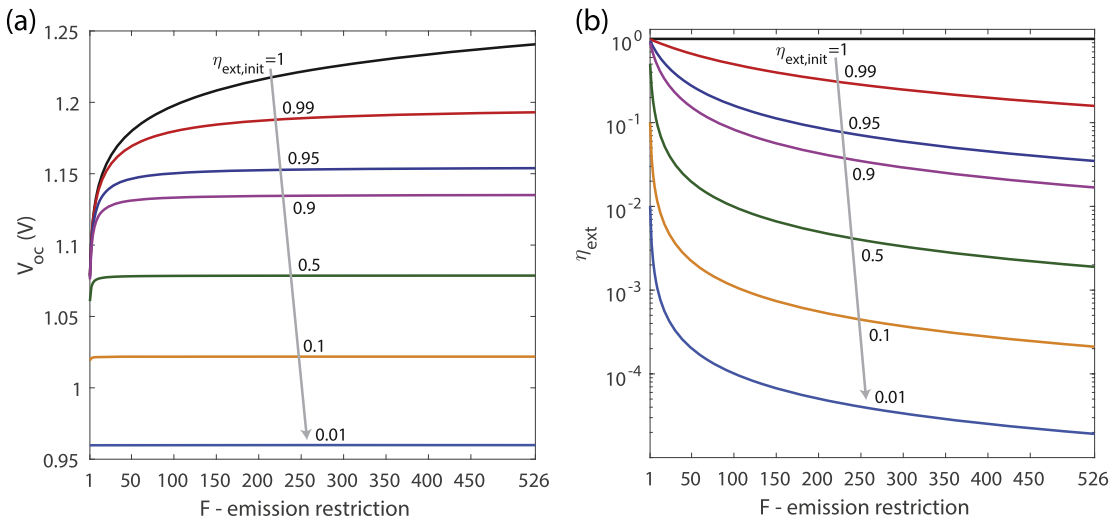

Figure 3. (a) Benefit of emission restriction on V_{oc}. Here, we consider a solar cell with $E_g = 1.34$ eV and we assume that emission occurs only to the top side, that is, $j_{em,ext,0,bot} = 0$. $F = 1$ corresponds to the case without emission restriction, in which case emission occurs at full emissivity to all angles at the top air side. $F = 526$ corresponds in turn to the case where the emission cone is restricted to match the incidence cone of 2.5° half angle of the AM1.5D solar spectrum. Here, we show results for varying initial $\eta_{ext,init}$, which is the value of η_{ext} at F = 1. (b) The drop in η_{ext} with increasing emission restriction F.

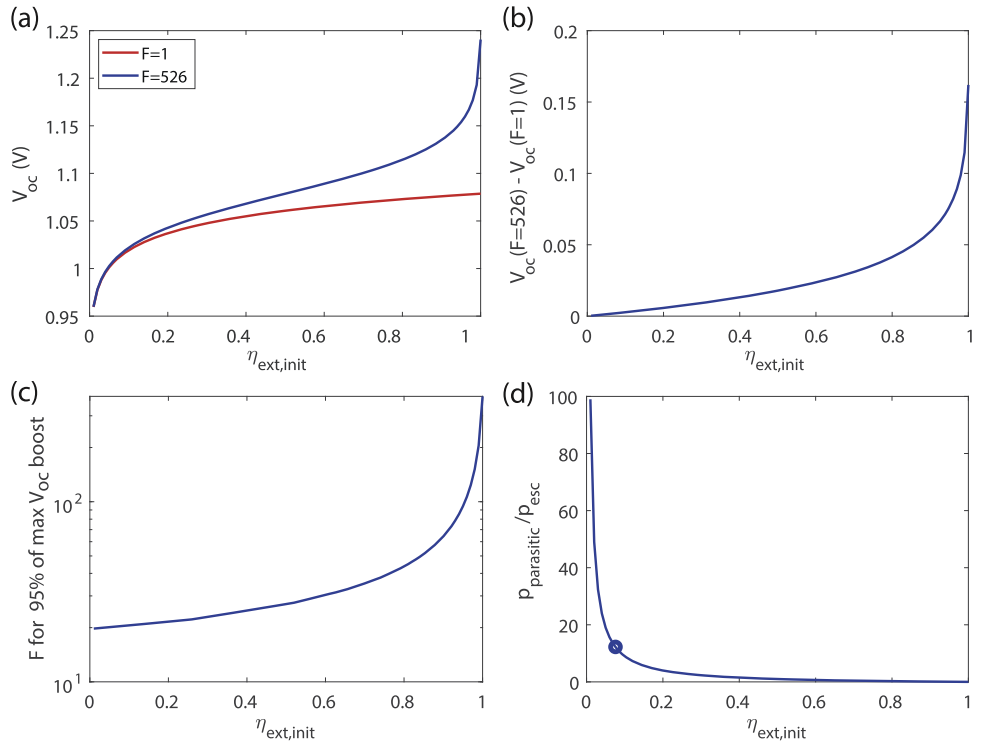

Figure 4. The same system as in figure 3. (a) V_{oc} for varying $\eta_{ext,init}$ that applies at $F = 1$. We show V_{oc} for $F = 1$ (no emission restriction) and $F = 526$ (full emission restriction). (b) The maximum boost in V_{oc} by emission restriction, which is given by the difference in V_{oc} at $F = 1$ and $F = 526$ shown in (a). (c) The emission restriction factor F that yields 95% of the maximum voltage boost at $F = 526$ shown in (b). (d) The relation between $\eta_{ext,init}$ and $p_{parasitic}/p_{esc}$ at $F = 1$ in the absence of non-radiative recombination.

by 15% from the initial V_{oc} of 1.08 V. We expect a similar relative increase in the solar cell efficiency η_{PV} (since we assume that j_{sc} stays constant), which in this case of a radiatively limited cell gives an increase from the conventional Shockley-Queisser limit of $\eta_{PV} \approx 33\%$ to $\eta_{PV} \approx 38\%$ (see figure 2(b) for the IV curve of the $\eta_{PV} \approx 33\%$ with $\eta_{ext} = 1$ and $F = 1$).

From figure 4(c) we see that for $\eta_{\mathrm{ext,init}} < 0.5$, it is enough with $F = 25$ to obtain 95% of the voltage boost obtained at the maximum $F = 526$. The requirement on F increases rapidly for $\eta_{\mathrm{ext,init}} > 0.9$, and for $\eta_{\mathrm{ext,init}} = 0.98$, $F = 200$ is needed to obtain 95% of the maximum voltage boost.

The $\eta_{\mathrm{ext,init}}$ is affected by both non-radiative recombination and parasitic absorption. As seen from equation (16), parasitic absorption and non-radiative recombination enter η_{ext} in the same manner. Then, assuming zero non-radiative recombination for the moment, that is, when $\eta_{\mathrm{int}} = 1$ and hence $j_{\mathrm{nr},0} = 0$, we can translate the initial $\eta_{\mathrm{ext,init}}$ to the initial ratio of $p_{\mathrm{parasitic}}/p_{\mathrm{esc}}$ shown in figure 4(d). Note that $p_{\mathrm{parasitic}}/p_{\mathrm{esc}} \to 0$ when $\eta_{\mathrm{ext,init}} \to 1$. In figure 4(d), the sphere marks the point $\frac{p_{\mathrm{parasitic}}}{p_{\mathrm{esc}}} = 3.5^2 = 12.25$ that corresponds to a fully absorbing back mirror in the ray-optics approximation, or alternatively to parasitic absorption in a refractive-index matched inactive substrate of the same $n = 3.5$ as the solar cell. In that case, $\eta_{\mathrm{ext}} = 0.0755$ and the maximum gain in V_{oc} is just 2 mV by restriction of the emission on the top side (figure 4(a)). Additional non-radiative recombination drops η_{ext} further from the values given by $\frac{p_{\mathrm{parasitic}}}{p_{\mathrm{esc}}}$ in figure 4(d), leading to even lower V_{oc} gain with the emission restriction on the top-side.

The above analysis of emission restriction, which reduces the recombination current $j_{\mathrm{rec}}(V)$, was done for non-concentrated sun light. In contrast, if external optics is used for concentrating sun light by a factor of C, which is expected to lead to a higher short-circuit current j_{sc} by a factor of C, the V_{oc} can obtain a boost, as seen from equation (14), even if η_{ext} is low due to strong non-radiative recombination or parasitic absorption [2, 9]. Note that in practice, with increasing C, heating of the cell and series resistance becomes increasingly limiting factors for the boost in V_{oc}. Note that when $\eta_{\mathrm{ext}} = 1$, that is, when all recombination is radiative and when no parasitic absorption occurs, there is equivalence between angle restriction of emission to reduce $j_{\mathrm{rec}}(V)$ and concentration of incident light to increase j_{sc}, where $C = F$ gives the same V_{oc} with the two approaches to increase V_{oc} [16] (see equation (14) where, j_{sc} would be increased by the factor of C or $j_{\mathrm{em,ext},0}$ decreased by the factor of F—note that for this case of $\eta_{\mathrm{ext}} = 1$, $j_{\mathrm{nr},0} = 0$ and $j_{\mathrm{parasitic},0} = 0$).

3.6. Direct versus diffuse incident light

Above, we focused on the 900 W m^{-2} AM1.5D direct and circumsolar solar spectrum for which the light is incident from a cone of 2.5° half angle [4]. In case we restrict the emission on the top side to match that incidence cone in order to enhance the V_{oc} as in figures 3 and 4, we should use a mechanical system to track the sun with the solar cell. Without solar tracking, for most of the day, the sun would be beyond the 2.5° incidence acceptance cone, and the cell would not generate any short-circuit current and hence no power.

Compared to the AM1.5D spectrum, the AM1.5G global tilt spectrum contains also sky and ground diffuse scattered light and has an intensity of 1000 W m^{-2} [4]. Hence, if we are in illumination conditions that follow the AM1.5G spectrum but use a sun-tracking cell optimized for the 2.5° half angle with zero absorption and emission outside of this cone, we expect to miss out on more than 99% of the 100 W m^{-2} of diffuse illumination (the 2.5° incidence cone corresponds approximately to $1/526 \approx 0.2\%$ of the light incident from the full hemisphere). This missing out of the diffuse light would reduce the j_{sc} potential by ≈10%, leading to a 10% relative decrease in the solar cell efficiency η_{PV}. The relative gain in V_{oc} enabled by the angle restriction outside of this 2.5° cone is on the other hand maximally 15% (at $\eta_{\mathrm{ext,init}} = 1$) and drops to 10% already at $\eta_{\mathrm{ext,init}} = 0.985$ (see figures 4(a) and (b)). Hence, if we don't absorb such diffuse light when present, we need a solar cell of extremely high external luminescence efficiency to gain in η_{PV} from the boost in V_{oc} due to angle restricting the emission of all above bandgap photons.

However, we could in principle tailor the emission/absorption properties such that the angle restriction applies only in a limited wavelength range close to the bandgap energy where the emission pre-dominantly occurs, whereas we could allow diffuse light of shorter wavelengths to still enter the solar cell for absorption [13], as long as we use a solar tracking system. For the below example analysis, we introduce a wavelength $\lambda_{\mathrm{restriction}}$ above which we restrict the angular emission. In terms of the absorptance and emissivity, $A_{\mathrm{top}}(\lambda, \theta, \phi, \mathrm{pol}) = e_{\mathrm{top}}(\lambda, \theta, \phi, \mathrm{pol}) = 1$ at all incidence angles for $\lambda < \lambda_{\mathrm{restriction}}$ to allow for absorption of the short-wavelength diffuse light, whereas for $\lambda_{\mathrm{restriction}} < \lambda < \lambda_{\mathrm{g}}$, $e_{\mathrm{top}}(\lambda, \theta, \phi, \mathrm{pol}) = 0$ for $\theta > 2.5°$ and $e_{\mathrm{top}}(\lambda, \theta, \phi, \mathrm{pol}) = 1$ for $\theta < 2.5°$ (for the calculation with angle dependent emissivity, we use equation (S3) in the supporting information; and for calculation of short-circuit current in equation (2), when $\lambda > \lambda_{\mathrm{restriction}}$ ($\lambda < \lambda_{\mathrm{restriction}}$) we use for $I_{\mathrm{inc}}(\lambda)$ the values given by the AM1.5D (AM1.5G) spectrum).

In figures 5 and 6, we show the benefit of such angle restriction around the bandgap energy. First, the short-circuit current j_{sc} drops monotonously as $\lambda_{\mathrm{restriction}}$ is decreased (figure 5(a)) since less and less of the diffuse light is utilized. As $\lambda_{\mathrm{restriction}}$ is decreased from 925 to 400 nm, the drop in j_{sc} is approximately 3 mA cm^{-2}, or 10% relative, close to the upper limit of 10% given by the fraction of diffuse light in the incident spectrum. In contrast, V_{oc} in figure 5(b) increases initially with decreasing $\lambda_{\mathrm{restriction}}$ since the emission of photons is restricted more and more. However, there appears a limit beyond which a decrease in $\lambda_{\mathrm{restriction}}$ does not appear to increase V_{oc}. This plateau region originates from the exponential decay of the emission with increasing photon energy (see

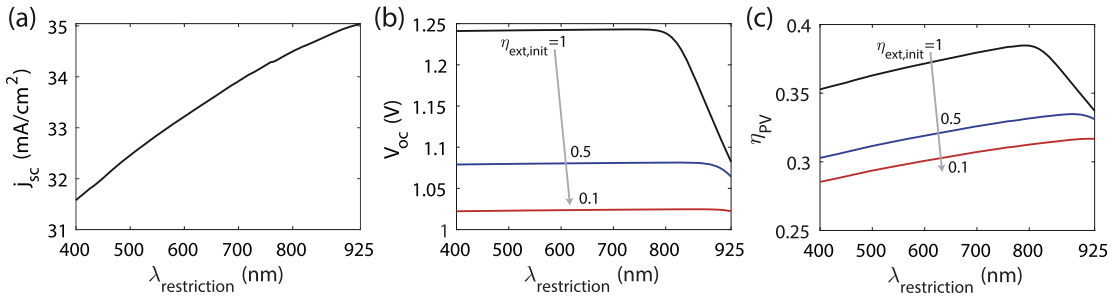

Figure 5. The dependence of (a) j_{sc}, (b) V_{oc}, and (c) η_{PV} on $\lambda_{restriction}$. We show results for varying initial external luminescence efficiency $\eta_{ext,init}$ that applies before any angle restriction. Note that j_{sc} does not depend on $\eta_{ext,init}$ under our assumptions. $\lambda_{restriction}$ denotes the wavelength above which the solar cell absorbs only from, and emit only to, the 2.5° half-angle incidence cone of the 900 W m^{-2} AM1.5D spectrum. For $\lambda < \lambda_{restriction}$, the solar cell absorbs diffuse light from the full top hemisphere and consecutively shows maximum emissivity to the full hemisphere. That is, for $\lambda < \lambda_{restriction}$, the solar cell absorbs light from the 1000 W m^{-2} AM1.5G spectrum, and for $\lambda_{restriction} < \lambda < \lambda_g = 925$ nm, the solar cell absorbs light from the 900 W m^{-2} AM1.5D spectrum; assuming negligible contribution from the diffuse light in the incidence cone of 2.5° half-angle.

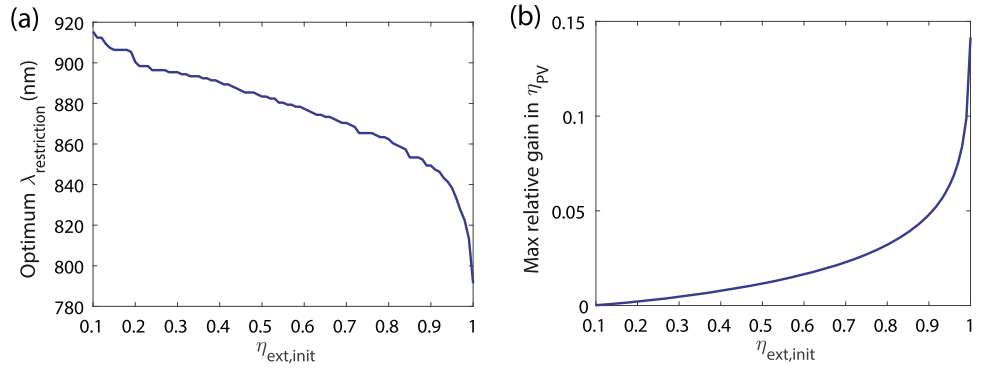

Figure 6. The same system as in figure 5. (a) Optimum $\lambda_{restriction}$ that gives the maximum relative increase in η_{PV} shown in (b). The rugged, fluctuating features in the optimum $\lambda_{restriction}$ originate from the rugged features in the incident AM1.5D/AM1.5G solar spectrum. (b) Maximum relative increase in η_{PV} by optimum choice of $\lambda_{restriction}$ compared to the case of no emission restriction.

figure 5 in [18]): a restriction of emissivity in a region with negligible emission to start with has negligible effect on the V_{oc}. Actually, there is instead a very minor decrease in V_{oc} with further decrease in $\lambda_{restriction}$ due to the decrease in j_{sc}. Note that with decreasing $\eta_{ext,init}$, there is less relative boost in V_{oc} by the emission-angle restriction. Then, the very minor decrease in V_{oc} due to the decreasing j_{sc} starts to dominate at a larger $\lambda_{restriction}$ over the increase due to emission restriction, and the on-set of the apparent plateau-region red-shifts with decreasing $\eta_{ext,init}$ as seen in figure 5(b).

Due to these opposing trends in V_{oc} and j_{sc} when $\lambda_{restriction}$ is decreased from the bandgap wavelength, a peak in η_{PV} shows up for some intermediate $\lambda_{restriction}$ (figure 5(c)). The value of this optimum $\lambda_{restriction}$ depends strongly on $\eta_{ext,init}$, the external luminescence efficiency before any angle restriction is applied (figure 6(a)). For small values of $\eta_{ext,init}$, the value of $\lambda_{restriction}$ is close to the bandgap wavelength of 925 nm. That is, in a solar cell that is strongly non-radiatively limited, we should simply aim to maximize j_{sc} by not using angle restriction at all. Also, the maximum relative gain in η_{PV} by such angle restriction shows strong dependence on $\eta_{ext,init}$. The maximum relative gain in η_{PV} shown in figure 6(b) is 14% and occurs at $\lambda_{restriction} = 790$ nm for $\eta_{ext,init} = 1$. The maximum relative gain drops to 3% at $\eta_{ext,init} = 0.8$ and to 1% for $\eta_{ext,init} = 0.5$.

Thus, there can be benefit of angle restricting the emission also when diffuse incident light is present. Such wavelength dependent angle restriction could be realized for example with a dielectric angle-restrictor multilayer, with which a 3.6 mV increase in V_{oc} has been demonstrated for a GaAs cell [13].

Note that there are conditions where the ratio of diffuse light intensity to direct light intensity can increase well past the expected 10% of the AM1.5G spectrum, for example due to cloudy weather or smog. In such cases, due to the stronger drop in j_{sc} with angle restriction, the benefit of angle restriction of emission, even if applied only around the bandgap, is expected to diminish even if η_{ext} is very high.

4. Conclusions

We performed a Shockley-Queisser detailed balance analysis of the benefit of external and internal management of emitted photons in a single-junction solar cell. We started from a diode-equation and connected the solar cell performance to the LED performance. In this way, we could predict the benefit of restricting the external emission of photons for varying internal and external luminescence efficiency. Specifically, we predicted a negligible practical benefit of managing externally emitted photons if the external luminescence efficiency is below 10%. Also, we connected the external emissivity to the probability that an internally emitted photon escapes the solar cell. Then, we could explain that we should minimize the probability that an internally emitted photon escapes, as long as we can ascertain that the photons that still manage to escape, escape into the cone from which light is incident from.

Here, we would like to point out that for design optimization, it could be important to be able to discriminate parasitic absorption from non-radiative recombination in order to know which process limits V_{oc} more. A measurement of η_{int} by temperature dependent electroluminescence measurements could shine light on the strength of the non-radiative recombination, but care must be taken to avoid artefacts, especially if considering a nanostructured solar cell due to a possible temperature dependence in p_{esc} [38].

In the end, we compared the benefit of managing the emission of photons for (i) the AM1.5D spectrum in which all light is incident at nearly normal angle and (ii) the AM1.5G global tilt spectrum for which we assumed 10% diffusively incident light. We showed that for such partially diffuse incident light, there can be an up to 14% relative boost in efficiency by emission management.

Acknowledgments

This work was supported by the Academy of Finland grant numbers 286920 and 315403. The authors would also like to thank the People Programme (Marie Curie Actions) of the European Union's Seventh Framework Programme (FP7-People-2013-ITN) under REA grant agreement No. 608153, PhD4Energy, and the European Union's Horizon 2020 research and innovation programme under grant agreement No. 641023, NanoTandem.

ORCID iDs

Nicklas Anttu https://orcid.org/0000-0002-7626-5107
Pyry Kivisaari https://orcid.org/0000-0001-8434-3438
Yang Chen https://orcid.org/0000-0002-8964-0084

References

[1] REN21 2018 R. global status report *Tech. Rep.* (Paris, France: REN21 Secretariat)
[2] Green M A, Hishikawa Y, Dunlop E D, Levi D H, Hohl-Ebinger J, Yoshita M and Ho-Baillie A 2019 Solar cell efficiency tables (version 53) *Prog. Photovolt. Res. Appl.* **27** 3–12
[3] Kirchartz T and Rau U 2018 What makes a good solar cell? *Adv. Energy Mater.* **8** 1703385
[4] ASTM G173-03 2012 Standard tables for reference solarspectral irradiances: direct normal and hemispherical on 37°tilted surface ASTM International, West Conshohocken, PA
[5] Shockley W and Queisser H J 1961 Detailed balance limit of efficiency of p-n junction solar cells *J. Appl. Phys.* **32** 510–9
[6] Yu Z, Raman A and Fan S 2010 Fundamental limit of nanophotonic light trapping in solar cells *PNAS* **107** 17491–6
[7] Yablonovitch E and Cody G D 1982 Intensity enhancement in textured optical sheets for solar cells *IEEE Trans. Electron. Dev.* **29** 300–5
[8] Green M A 1982 Accuracy of analytical expressions for solar cell fill factors *Sol. Cells* **7** 337–40
[9] Araújo G L and Martí A 1994 Absolute limiting efficiencies for photovoltaic energy conversion *Solar Energy Mater. Solar Cells* **33** 213–40
[10] Ganapati V, Steiner M A and Yablonovitch E 2016 The voltage boost enabled by luminescence extraction in solar cells *IEEE J. Photovolt.* **6** 801–9
[11] Cui Y, van Dam D, Mann S A, van Hoof N J J, van Veldhoven P J, Garnett E C, Bakkers E P A M and Haverkort J E M 2016 Boosting solar cell photovoltage via nanophotonic engineering *Nano Lett.* **16** 6467–71
[12] Steiner M A, Geisz J F, Garcia I, Friedman D J, Duda A, Olavarria W J, Young M, Kuciauskas D and Kurtz S 2013 Effects of internal luminescence and internal optics on V_{oc} and J_{sc} of III–V solar cells *IEEE J. Photovolt.* **3** 1437–42
[13] Kosten E D, Kayes B M and Atwater H A 2014 Experimental demonstration of enhanced photon recycling in angle-restricted GaAs solar cells *Energy & Env. Sci.* **7** 1907–12
[14] Miller O D, Yablonovitch E and Kurtz S 2012 Strong internal and external luminescence as solar cells approach the Shockley-Queisser limit *IEEE J. Photovolt.* **2** 303–11
[15] Munday J N 2012 The effect of photonic bandgap materials on the Shockley-Queisser limit *J. Appl. Phys.* **112** 064501
[16] Rau U, Paetzold U W and Kirchartz T 2014 Thermodynamics of light management in photovoltaic devices *Phys. Rev.* B **90** 035211
[17] Steiner M, Geisz J, Garcia I, Friedman D, Duda A and Kurtz S 2013 Optical enhancement of the open-circuit voltage in high quality GaAs solar cells *J. Appl. Phys.* **113** 123109
[18] Anttu N 2015 Shockley-Queisser detailed balance efficiency limit for nanowire solar cells *ACS Photonics* **2** 446–53

[19] Xu Y, Gong T and Munday J N 2015 The generalized Shockley-Queisser limit for nanostructured solar cells *Sci. Rep.* **5** 13536
[20] Sandhu S, Yu Z and Fan S 2013 Detailed balance analysis of nanophotonic solar cells *Opt. Express* **21** 1209–17
[21] Rau U 2007 Reciprocity relation between photovoltaic quantum efficiency and electroluminescent emission of solar cells *Phys. Rev.* B **76** 085303
[22] Abebe M G, Abass A, Gomard G, Zschiedrich L, Lemmer U, Richards B S, Rockstuhl C and Paetzold U W 2018 Rigorous wave-optical treatment of photon recycling in thermodynamics of photovoltaics: perovskite thin-film solar cells *Phys. Rev.* B **98** 075141
[23] Haverkort J E, Garnett E C and Bakkers E P 2018 Fundamentals of the nanowire solar cell: optimization of the open circuit voltage *Appl. Phys. Rev.* **5** 031106
[24] Chen Y, Kivisaari P, Pistol M and Anttu N 2017 Optimized efficiency in InP nanowire solar cells with accurate 1D analysis *Nanotechnology* **29** 045401
[25] Anttu N 2019 Physics and design for 20% and 25% efficiency nanowire array solar cells *Nanotechnology* **30** 074002
[26] Toprasertpong K, Delamarre A, Nakano Y, Guillemoles J and Sugiyama M 2019 Generalized reciprocity relations in solar cells with voltage-dependent carrier collection: application to p-i-n junction devices *Physi. Rev. Appl.* **11** 024029
[27] Lu N, Li L, Sun P and Liu M 2014 Short-circuit current model of organic solar cells *Chem. Phys. Lett.* **614** 27–30
[28] Xu G, Lu N, Wang W, Gao N, Ji Z, Li L and Liu M 2015 Universal description of exciton diffusion length in organic photovoltaic cell *Org. Electron.* **23** 53–6
[29] Lu N, Wang J, Geng D, Li L and Liu M 2019 Understanding the transport mechanism of organic-inorganic perovskite solar cells: the effect of exciton or free-charge on diffusion length *Org. Electron.* **66** 163–8
[30] Wallentin J *et al* 2013 InP nanowire array solar cells achieving 13.8% efficiency by exceeding the ray optics limit *Science* **339** 1057–60
[31] Åberg I, Vescovi G, Asoli D, Naseem U, Gilboy J P, Sundvall C, Dahlgren A, Svensson K E, Anttu N and Björk M T 2016 A GaAs nanowire array solar cell with 15.3% efficiency at 1 sun *IEEE J. Photovolt.* **6** 185–90
[32] Otnes G, Barrigón E, Sundvall C, Svensson K E, Heurlin M, Siefer G, Samuelson L, Åberg I and Borgström M T 2018 Understanding InP nanowire array solar cell performance by nanoprobe-enabled single nanowire measurements *Nano Lett.* **18** 3038–33046
[33] Robinson S, Aberle A and Green M 1994 Departures from the principle of superposition in silicon solar cells *J. Appl. Phys.* **76** 7920–30
[34] Anttu N 2016 Connection between modeled blackbody radiation and dipole emission in large-area nanostructures *Opt. Lett.* **41** 1494–7
[35] Wurfel P 1982 The chemical potential of radiation *J. Phys.* C **15** 3967
[36] Mattheis J, Werner J H and Rau U 2008 Finite mobility effects on the radiative efficiency limit of p n-junction solar cells *Phys. Rev.* B **77** 085203
[37] Markvart T 2018 Reciprocity and open-circuit voltage in solar cells *IEEE J. Photovolt.* **8** 67–9
[38] Kivisaari P, Chen Y and Anttu N 2018 Emission enhancement, light extraction and carrier dynamics in InGaAs/GaAs nanowire arrays *Nano Futures* **2** 015001